DESIGN AND EVALUATION OF THERMAL STORAGE INTEGRATED SOLAR DRYER WITH ABSORBER PLATES

Anilgandhi Gottipalli[1], Mrs. K. Chandana[2], Mr. Dosapati Chaitanya[3]

[1]PG Scholar, Department of Mechanical Engineering, Visakha Institute of Engineering & Technology (Autonomous)
Visakhapatnam, Andhra Pradesh - 530027, India

[2]Assistant Professor, Department of Mechanical Engineering, Visakha Institute of Engineering & Technology (Autonomous)
Visakhapatnam, Andhra Pradesh - 530027, India

[3]Assistant Professor, Department of Mechanical Engineering, Andhra Pradesh, India

Abstract

Solar energy is one of the most abundant and environmentally sustainable renewable resources available for thermal applications. Solar air heaters (SAHs) are widely used for space heating, crop drying, and industrial thermal processes owing to their simple construction and low operating cost; however, their thermal performance is often limited by low convective heat transfer rates and the intermittent nature of solar radiation. This paper presents the design, fabrication, and experimental evaluation of a thermal-storage-integrated solar dryer that employs aluminium absorber plates coupled with a Phase Change Material (PCM). Two absorber-cum-storage geometries were developed and tested under identical outdoor conditions: a Rhombus Wax Storage Unit (RWSU) and an Aerofoil Wax Storage Unit (AWSU), both fabricated from aluminium sheet and filled with paraffin wax as the latent-heat storage medium. Parameters including inlet and outlet air temperature, absorber and PCM temperature, solar irradiance, air mass flow rate, and pressure differential were recorded over multiple test days and used to compute the instantaneous and average thermal efficiency of each configuration. The results show that PCM integration considerably improves temperature stability and extends useful heating beyond periods of peak insolation. Both geometries enhanced heat transfer relative to a plain absorber; however, the aerofoil configuration consistently achieved higher average thermal efficiency (up to 49.0%) due to its streamlined profile, larger convective surface area, and lower flow resistance compared with the rhombus configuration (up to 47.5%). The findings confirm that combining an aerodynamic absorber geometry with PCM-based thermal storage is an effective, low-cost strategy for improving the performance of solar air heaters used in agricultural drying and other low-temperature thermal applications.

Keywords—*Solar Air Heater; Phase Change Material; Paraffin Wax; Aerofoil Absorber; Rhombus Storage Unit; Thermal Efficiency; Thermal Energy Storage; Solar Drying.*

Nomenclature

Symbol	Description	Symbol	Description
SAH	Solar air heater	Q	Volumetric flow rate (m^3/s)
Ti (°C)	Inlet air temperature	$\dot{m}$	Mass flow rate (kg/s)
To (°C)	Outlet air temperature	Qu	Useful heat gain (W)
Tabs (°C)	Absorber plate temperature	QPCM	Heat storage rate of PCM

Symbol	Description	Symbol	Description
I	Solar irradiance (W/m²)	Tmelt	Melting temperature of PCM
Cp	Specific heat of air	L	Latent heat of fusion (J/kg)
Ac	Collector aperture area (m²)	η	Thermal efficiency
d, D	Orifice / pipe diameter	β	Diameter ratio, d/D
ΔP	Pressure head difference (Pa)	ρ	Fluid density (kg/m³)
Cd	Coefficient of discharge	U	Expanded uncertainty (±2σ)

1. Introduction

India occupies a premier position on the global solar map, benefiting from a geographical location that provides an average solar insolation of 4 to 7 kWh/m²/day. With the Government of India targeting 500 GW of installed renewable energy capacity by 2030, the transition from fossil-fuel-dependent heating to solar-thermal solutions has become a critical step toward reducing greenhouse-gas emissions and achieving long-term energy security. Solar thermal technology offers a direct and efficient route to these goals by bypassing the conversion losses associated with photovoltaic-to-electrical routes.

A Solar Air Heater (SAH) is a thermal device that captures incident solar radiation and transfers the resulting heat to air flowing through the collector. Unlike solar water heaters, SAHs use air as the working fluid, which eliminates problems such as freezing, corrosion, and leakage. Owing to their simple construction, low maintenance, and low cost, SAHs are widely used for space heating, crop and food-grain drying, timber seasoning, and industrial drying operations. The basic structure of an SAH consists of a transparent glazing cover, an absorber plate, an insulated duct, and an air-circulation mechanism. Solar radiation passes through the glazing and is absorbed by the plate; the absorbed heat is then transferred by convection to the air flowing beneath or over the plate, raising its temperature before it leaves the collector.

The thermal efficiency of a conventional flat-plate SAH is fundamentally limited by the low thermal conductivity and heat capacity of air, and by the development of a thermal boundary layer on the absorber surface, which acts as an insulating film and restricts heat transfer. Surface modifications such as ribs, fins, baffles, and specially shaped storage units are commonly introduced to disrupt this boundary layer, increase the effective heat-transfer area, and promote turbulence. In addition, because solar radiation is intermittent and unavailable after sunset, Thermal Energy Storage (TES) using a Phase Change Material (PCM) is increasingly used to store surplus heat during periods of high insolation and release it gradually when radiation is low, thereby stabilising the outlet air temperature and extending the useful operating window of the collector.

The present work integrates both strategies — a heat-transfer-enhancing absorber geometry and PCM-based thermal storage — into a single hybrid solar dryer. Two absorber-storage geometries filled with paraffin wax are proposed and compared: (i) a Rhombus Wax Storage Unit (RWSU), whose sharp inclined faces are intended to generate strong flow disturbances and turbulence, and (ii) an Aerofoil Wax Storage Unit (AWSU), whose streamlined, symmetric profile is intended to enhance convective area while minimising pressure drop. Aluminium was selected as the fabrication material for both the absorber plate and the storage units because of its high thermal conductivity, low weight, and corrosion resistance. The objective of the study is to fabricate both configurations, test them experimentally under outdoor solar conditions, and quantitatively compare their thermal performance so as to identify the more effective geometry for solar-drying applications.

2. Literature Survey

The development of high-efficiency solar air heaters has attracted considerable research attention due to the growing demand for sustainable thermal-energy systems. Prior studies have investigated absorber-plate modifications, artificial roughness elements, fin geometries, flow configurations, and PCM-based storage to improve collector performance; a representative summary is given below.

Nagaraj et al. [1] carried out a numerical study on a single-flow double-pass SAH with aerofoil fins over a Reynolds-number range of 3,000–24,000 and reported that an alternative aerofoil-fin arrangement with a 10 mm fin height gave a thermal efficiency about 23.2% higher than the baseline single-pass model, with a 20.9% improvement in thermo-hydraulic efficiency. Santh et al. [2] compared six collector-plate geometries in an indirect solar dryer and found that an alternative wing-type absorber achieved a maximum Nusselt number of 53.8 — more than twice that of a flat plate — although at the cost of a higher friction factor. Singh et al. [3] reviewed recent developments in SAH technology and identified the multi-V-shaped rib as one of the most effective roughness geometries, while noting that double-pass parallel-flow configurations combine high heat-transfer efficiency with reduced drag.

Dosapati et al. [4] experimentally studied a packed-bed double-pass SAH with encapsulated PCM storage and reported that the practical efficiency of the PCM-based thermal-storage unit was 22% higher during charging and 6% higher during discharging than an equivalent unit with a plain absorber. Al-Sulaiman et al. [5] analysed a double-pass SAH integrated with a PCM-based thermal-storage unit and found that the storage system extended heat retention and stabilised the outlet air temperature well beyond sunshine hours. Machi [6] reported that triangular fins on a double-pass collector improved daily efficiency by 4–6% relative to a flat absorber, while Murali et al. [7] found that longitudinal aluminium fins placed in the lower channel of a double-pass collector outperformed an upper-channel placement by 4–17%, reaching a peak efficiency of 78%.

Sahu and Prasad [8] showed that arc-shaped wire-rib roughness on the absorber plate can raise exergy efficiency by up to 56% relative to a smooth absorber, with an optimum near a Reynolds number of 10,000–12,000. Chabane et al. [9] found that rectangular baffle fins placed directly beneath the absorber plate achieved a thermal efficiency of 58% at a solar intensity of 937 W/m², outperforming both bottom-plate baffle placement and a smooth duct. Finally, Khan et al. [10] reviewed heat-transfer-intensification techniques for latent-heat thermal-storage systems and concluded that, while extended fin surfaces remain the most cost-effective enhancement, high-conductivity metal-foam inserts and nano-additives dispersed in the PCM offer superior thermal performance by creating continuous high-conductivity paths through the otherwise poorly conducting PCM.

Ref.	Enhancement Technique	Key Reported Result
[1]	Aerofoil fins, double pass	+23.2% efficiency vs. baseline
[2]	Alternative wing absorber	Nu = 53.8 (2.6× flat plate)
[3]	Multi-V rib roughness	Reduced drag, high efficiency
[4]	Encapsulated PCM, packed bed	+22% (charge), +6% (discharge)
[5]	PCM-based TES, double pass	Stabilised outlet temperature
[6]	Triangular fins	+4–6% daily efficiency
[7]	Longitudinal fins (lower ch.)	78% peak efficiency
[8]	Arc-shaped wire rib	+56% exergy efficiency
[9]	Rectangular baffle fins	58% at 937 W/m²

Ref.	Enhancement Technique	Key Reported Result
[10]	Fins / metal foam in PCM	Higher conductivity path

TABLE I. SUMMARY OF REVIEWED HEAT-TRANSFER ENHANCEMENT STUDIES

Collectively, the reviewed literature establishes two consistent findings that motivate the present work: (i) streamlined or aerodynamically shaped absorber/fin geometries provide a favourable balance between enhanced heat transfer and limited pressure drop, and (ii) PCM-based thermal storage is highly effective at mitigating the intermittency of solar radiation. However, comparatively few studies directly compare a streamlined aerofoil geometry against a turbulence-promoting angular geometry under identical PCM loading and outdoor test conditions — the gap addressed in this study.

3. Existing System

Conventional solar drying systems can be broadly classified as direct (natural-convection cabinet) dryers, indirect (forced or natural-convection SAH-fed) dryers, and mixed-mode dryers that combine direct solar exposure of the product with a separate SAH. Among these, indirect solar dryers coupled to a flat-plate SAH are the most widely deployed for agricultural and food-grain drying because the product is not directly exposed to solar radiation, dust, or insects, while the heated air supplied by the collector provides controlled, uniform drying.

The conventional flat-plate SAH used in most existing indirect dryers consists of a plain absorber plate (typically painted black or coated with a selective absorbing coating), a single or double glazing cover, an insulated back and side panel, and a duct through which air is moved by natural or forced convection. While such systems are simple, low-cost, and easy to fabricate, they suffer from well-documented limitations:

- Low convective heat-transfer coefficient between the plain absorber surface and the air stream, since air has inherently low thermal conductivity and heat capacity.
- Formation of a thermal and hydrodynamic boundary layer on the flat absorber surface, which acts as an insulating film and restricts further heat transfer to the bulk air flow.
- Strong dependence on instantaneous solar radiation — performance drops sharply during cloud cover and ceases almost entirely after sunset, since a conventional flat-plate collector has no significant heat-storage capacity.
- Non-uniform drying air temperature over the course of the day, which can lead to case-hardening, under-drying, or extended drying times for agricultural produce.

Some existing systems attempt to overcome the first two limitations by introducing artificial roughness (ribs, wire meshes, or baffles) on the absorber surface, which increases turbulence and heat-transfer area but simultaneously increases pumping-power requirements due to the higher pressure drop. Other existing systems attempt to overcome the third and fourth limitations by adding sensible-heat storage media such as pebble beds or gravel beds beneath the absorber plate; however, sensible storage media require a large mass and volume to store a comparatively modest amount of heat and typically show a large temperature swing between the charging and discharging phases.

The system proposed in this work is designed specifically to overcome these existing-system limitations simultaneously: heat-transfer area and turbulence are increased through a shaped (rhombus or aerofoil) absorber-storage geometry rather than simple roughness elements, and thermal storage is achieved using a compact, high-energy-density PCM (paraffin wax) rather than a bulky sensible-storage bed, so that a near-constant outlet air temperature can be sustained for a longer period after the peak insolation hours.

In terms of PCM selection, existing thermal-storage retrofits for SAHs have used a range of organic and inorganic materials, including paraffin wax, stearic acid, and various salt hydrates. Paraffin wax was selected for the present system because of its chemically stable, non-corrosive, and non-toxic behaviour, its congruent melting characteristics (melting without significant phase segregation), a melting point in a range suitable for low-temperature drying applications (approximately 50 °C, consistent with the PCM temperatures observed during testing), and its relatively low cost and wide commercial availability compared with more exotic PCM formulations. These properties make paraffin wax a practical, low-risk choice for a first-generation hybrid absorber-storage retrofit of an otherwise conventional flat-plate solar air heater.

4. Research Methodology

The proposed solar dryer uses a flat aluminium absorber plate of size 1100 mm × 800 mm, selected for its high thermal conductivity and corrosion resistance. To overcome the intermittency of solar collection, a dual-layer PCM containment strategy is used: a Rhombus-shaped Wax Storage Unit (RWSU) forms a base layer of latent-heat storage, further augmented in a separate test configuration by an array of hollow, three-dimensional Aerofoil-shaped Wax Storage Units (AWSU). Both units are fabricated from aluminium sheet and filled with paraffin wax, which functions as the PCM, absorbing surplus heat during peak solar noon (melting/charging) and releasing it to the airflow during periods of reduced radiation (solidifying/discharging).

A. Experimental Components

The experimental rig consists of the following major components: (i) a centrifugal air blower providing controlled forced convection through the duct at four to five selectable speed settings; (ii) a solar radiation (pyranometer-type) meter to record instantaneous insolation in W/m²; (iii) K-type thermocouples positioned at the inlet, outlet, absorber plate, PCM core, and upper/lower glazing surfaces; (iv) a hand-held digital anemometer to measure air velocity; (v) a digital micro-manometer to record the differential pressure across an orifice plate used for air-flow-rate measurement; and (vi) a transparent single-glazing cover mounted above the absorber duct.

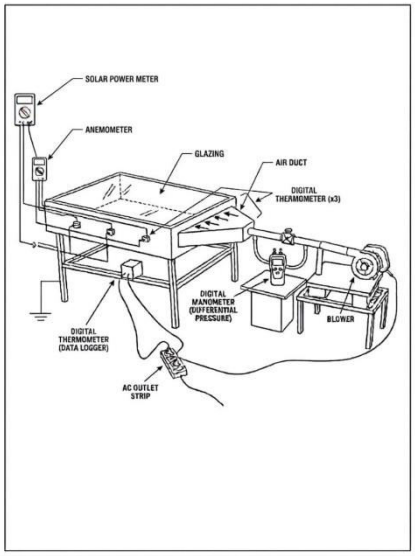

Fig. 1. Schematic layout of the solar air heater / dryer test rig.

B. Absorber Geometry and Fabrication

The Aerofoil Wax Storage Unit is designed using a symmetrical profile inspired by the standard NACA 0012 section. Because the original NACA 0012 dimensions (chord ≈ 80 mm, span ≈ 200 mm, thickness ≈ 9.6 mm) are too small to provide adequate PCM volume and heat-transfer area for a thermal prototype, the geometry was scaled up while preserving the symmetric shape and smooth curvature. The final aerofoil unit has a chord length of 165 mm, a span of 60 mm, and a maximum thickness of 40 mm, forming a hollow three-dimensional aerofoil that simultaneously acts as an extended heat-transfer surface and a PCM container. The AWSUs were arranged in a staggered array along the absorber plate to condition the airflow path and were fabricated by bending 2 mm thick aluminium sheet around a wooden bending mandrel machined to the exact internal aerofoil

profile, ensuring dimensional consistency across all units.

The Rhombus Wax Storage Unit was likewise fabricated from aluminium sheet; its inclined faces are intended to promote flow separation and reattachment, increasing turbulence intensity and thermal mixing relative to a plain absorber. After fabrication, both types of storage units were securely bonded to the absorber plate. Each rhombus unit was filled with 20 ml of paraffin wax (75% of internal volume) while each aerofoil unit was filled with 190 ml (also 75% of its larger internal volume); the 75% fill ratio was deliberately chosen to allow roughly 10–15% volumetric expansion during melting while still maximising latent-heat storage capacity.

Fig. 2. Fabricated Rhombus Wax Storage Unit (RWSU) bonded to the absorber plate.

Fig. 3. Wax-filled Aerofoil Wax Storage Unit (AWSU).

Table II lists the principal design and material specifications of the absorber plate and the two storage-unit geometries used in the experimental campaign.

Parameter	RWSU	AWSU
Base material	Aluminium sheet	Aluminium sheet (2 mm)
Absorber plate size	1100 × 800 mm	1100 × 800 mm
Unit profile	Rhombus (angular)	NACA 0012-based aerofoil
Chord / span / thickness	—	165 / 60 / 40 mm
PCM used	Paraffin wax	Paraffin wax
PCM fill volume / unit	20 ml (75%)	190 ml (75%)
Arrangement	Distributed array	Staggered array

TABLE II. ABSORBER / PCM STORAGE-UNIT SPECIFICATIONS

C. Thermal Analysis

Air-flow measurement is based on the orifice-meter method. The orifice and pipe cross-sectional areas are first obtained from their respective diameters, $A_o = \pi d^2/4$ and $A_p = \pi D^2/4$, and the diameter ratio $\beta = d/D$ is then used in the volumetric-flow-rate equation:

$$Q = C_d \cdot A_o \cdot \sqrt{[2\Delta P / (\rho(1 - \beta^4))]}$$

where Q is the volumetric flow rate (m^3/s), C_d is the discharge coefficient, A_o is the orifice area (m^2), ΔP is the differential pressure (Pa), ρ is air density (kg/m^3), and β is the orifice-to-pipe diameter ratio. The mass flow rate is then obtained as $\dot{m} = \rho Q$, and the useful heat gained by the air stream is calculated from $Q_u = \dot{m} \cdot C_p \cdot (T_o - T_i)$, where C_p is the specific heat of air and T_i, T_o are the inlet and outlet air temperatures, respectively.

The thermal energy stored within the PCM, accounting for both sensible and latent components, is given by $Q_{PCM} = m_{PCM}[C_{ps}(T_m - T_a) + L + C_{pl}(T_f - T_m)]$, where m_{PCM} is the mass of PCM, C_{ps} and C_{pl} are the specific heats of the solid and liquid phases, L is the latent heat of fusion, and T_m, T_a, T_f are the melting, initial, and final temperatures respectively. The instantaneous thermal efficiency of the collector is then evaluated as $\eta = Q_u / (I \cdot A_c)$, where I is the measured solar irradiance (W/m^2) and A_c is the collector aperture area (m^2).

Fig. 4. Fabricated experimental solar dryer test rig.

D. Thermocouple Calibration

All thermocouples were calibrated against a standard mercury-in-glass thermometer prior to testing, over a temperature range representative of the expected operating conditions. Table III summarises the calibration data; the mean error, standard deviation, and expanded uncertainty ($U = \pm 2\sigma$) were computed from the recorded deviations to establish the measurement confidence of the instrumentation used throughout the experimental campaign.

Std. Temp. Ts (°C)	Measured Tm (°C)	Error (°C)
25	26.10	+1.10
44	43.375	−0.625
56	56.3125	+0.3125
52	51.275	−0.725
58	58.3125	+0.3125
62	62.975	+0.975

TABLE III. THERMOCOUPLE CALIBRATION DATA

The experimental procedure was repeated identically for both the RWSU and AWSU configurations: the rig was oriented for maximum solar exposure, the blower was switched on to establish the required air-flow rate, and solar irradiance, all thermocouple temperatures, air velocity, and differential pressure were logged at 10-minute intervals throughout each test day. On selected days, logging was continued after 4:00 PM without insolation to isolate and quantify the heat-storage (discharging) contribution of the PCM.

5. Results and Discussions

The experimental campaign compared the thermal performance of the solar dryer under two absorber-storage configurations — the aluminium Rhombus Wax Storage Unit (RWSU) and the aluminium Aerofoil Wax Storage Unit (AWSU) — both filled with paraffin wax PCM. In each test, the outlet air temperature (To) was monitored as a function of the varying inlet air temperature (Ti) and instantaneous solar irradiance, and the thermal efficiency was calculated from the useful heat gain relative to the incident solar energy on the collector aperture.

A. Rhombus Wax Storage Unit (RWSU) Performance

Table IV summarises the four RWSU test days conducted at increasing blower speeds (Level 1 to Level 4). On Day 1 (lowest flow rate, 0.00040 kg/s), the inlet temperature rose from 29 °C to 33 °C while the outlet temperature increased from 37.4 °C to a peak of 50.0 °C, yielding an average thermal efficiency of 18.98%. As the mass flow rate was progressively increased on Days 2–4, the average thermal efficiency rose accordingly, reaching 24.72%, 31.09%, and a maximum of 47.46% on Day 4 at the highest tested flow rate of 0.00780 kg/s. This trend confirms that increasing the air-flow rate improves convective heat extraction from the rhombus storage unit, despite the correspondingly higher turbulence-induced pressure drop generated by its angular geometry. On Days 2–4, testing was extended beyond 4:00 PM without insolation; the outlet air temperature remained measurably above ambient during this period, confirming that the PCM continued to release stored latent heat after sunset conditions were simulated.

Day	Blower Lvl.	Ti range (°C)	To range (°C)	$\dot{m}$ (kg/s)	$\bar{\eta}$ (%)
1	1	29 → 33	37.4 → 50.0	0.00040	18.98
2	2	28 → 31	41.4 → 51.0	0.00411	24.72
3	3	27 → 29	31.5 → 56.7	0.00641	31.09

Day	Blower Lvl.	Ti range (°C)	To range (°C)	ṁ (kg/s)	η̄ (%)
4	4	23 → 28	40.3 → 55.9	0.00780	47.46

TABLE IV. RWSU DAY-WISE TEST SUMMARY

B. Aerofoil Wax Storage Unit (AWSU) Performance

Table V summarises the seven AWSU test days. The AWSU achieved a higher efficiency than the RWSU on the corresponding low-flow-rate days (23.06% on Day 1 versus 18.98% for RWSU, and 30.96% on Day 2 versus 24.72% for RWSU), reflecting the larger convective surface area and lower flow resistance of the streamlined aerofoil profile. Day 4 (0.00945 kg/s) produced the highest recorded efficiency of the entire study, 49.03%, exceeding the RWSU maximum of 47.46%. Day 5 was conducted under partially cloudy conditions at blower Level 5, with solar irradiance between 697 and 814 W/m²; even so, the outlet temperature reached 45.9 °C and the PCM temperature rose to approximately 60 °C, confirming a phase-change response, although the average efficiency for that day (20.07%) was reduced by the intermittent cloud cover. Days 6 and 7 exhibited stable moderate efficiencies of 26.46% and 33.65% respectively, at mass flow rates around 0.0078–0.0081 kg/s.

Day	Blower Lvl.	Ti range (°C)	To range (°C)	ṁ (kg/s)	η̄ (%)
1	—	26 → 27	29.8 → 31.4	0.00572	23.06
2	—	25 → 28	30.3 → 38.9	0.00761	30.96
3	—	27 → 29	31.6 → 38.5	0.00754	19.97
4	—	24 → 27	33.4 → 40.2	0.00945	49.03
5	5	—	— → 45.9	0.0069–0.0099*	20.07
6	—	23 → 28	31.8 → 43.4	0.00810	26.46
7	—	23 → 28	30.4 → 43.7	0.00780	33.65

TABLE V. AWSU DAY-WISE TEST SUMMARY (* range across test window)

C. Comparative Discussion

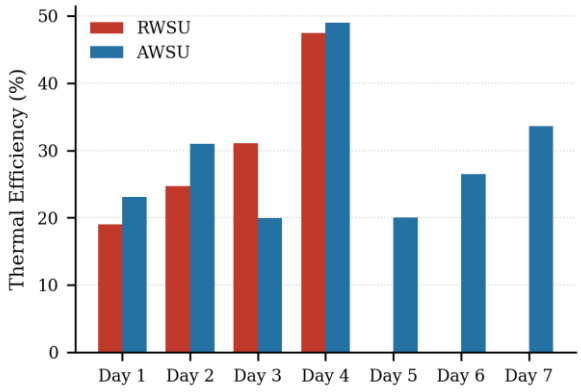

Fig. 5. Day-wise average thermal efficiency: RWSU vs. AWSU.

Figure 5 compares the average daily thermal efficiency achieved by the two configurations. Although the RWSU produced strong turbulence and comparable peak efficiency at the highest tested flow rate, its performance at low-to-moderate flow rates was consistently lower than that of the AWSU, and RWSU testing was limited to four days due to the higher pressure drop restricting the practical operating range of the blower. The AWSU, by contrast, sustained favourable efficiencies across a wider range of flow rates and delivered the single highest efficiency recorded in the study (49.03%), while also demonstrating a clear PCM charging/discharging response evidenced by elevated outlet temperatures during the post-insolation test window.

These observations are consistent with the underlying heat-transfer mechanisms: the rhombus geometry relies primarily on flow separation and turbulence generation to strip heat from the absorber surface, which is effective but comes at the cost of increased pumping power; the aerofoil geometry instead

relies on an enlarged, streamlined convective surface combined with reduced wake formation, allowing efficient heat exchange with substantially lower flow resistance. The larger internal PCM volume of the aerofoil unit (190 ml per unit versus 20 ml for the rhombus unit) also contributes to a greater latent-heat storage capacity, which explains the more pronounced and sustained post-sunset temperature elevation observed for the AWSU configuration. Overall, the results indicate that the Aerofoil Wax Storage Unit offers the more favourable combination of thermal efficiency, flow-resistance characteristics, and thermal-storage capacity for solar-dryer applications.

D. Measurement Uncertainty

The mean error, standard deviation, and expanded uncertainty of the temperature-measurement chain were evaluated from the calibration data in Table III using $\bar{e} = \Sigma e/n$ for the mean error, $\sigma = \sqrt{[\Sigma(e - \bar{e})^2 / (n - 1)]}$ for the standard deviation, and $U = \pm 2\sigma$ for the expanded uncertainty at approximately the 95% confidence level. The resulting uncertainty band was found to be small relative to the temperature differentials (Ti − To) recorded during testing, indicating that the day-to-day and configuration-to-configuration differences in thermal efficiency reported in Tables IV and V reflect genuine differences in thermal performance between the RWSU and AWSU geometries rather than measurement noise.

6. Conclusion

A thermal-storage-integrated solar dryer employing PCM-filled aluminium absorber units was designed, fabricated, and experimentally evaluated using two storage geometries — the Rhombus Wax Storage Unit (RWSU) and the Aerofoil Wax Storage Unit (AWSU). Based on the experimental observations, the following conclusions are drawn:

- Integration of paraffin-wax PCM significantly enhanced the thermal-storage capability of the solar air heater, allowing excess solar energy collected during peak sunshine hours to be released during low-radiation periods and after simulated sunset conditions.
- Both the RWSU and the AWSU improved heat-transfer performance relative to a conventional flat absorber plate, and the outlet air temperature remained consistently higher than the inlet temperature throughout testing, confirming effective heat absorption and transfer in both configurations.
- The RWSU generated strong airflow turbulence, enhancing convective heat transfer but at the cost of higher pressure drop and a narrower practical operating range.
- The AWSU provided improved airflow characteristics due to its streamlined geometry, reducing pressure losses while sustaining efficient heat transfer across a wider range of flow rates.
- The AWSU achieved the highest overall thermal efficiency recorded in the study (49.03%), compared with a maximum of 47.46% for the RWSU, owing to its larger heat-transfer surface area, greater PCM volume, and more favourable airflow distribution.
- The proposed hybrid absorber/PCM system offers a simple, economical, and environmentally friendly means of improving solar-air-heater performance and is well suited to agricultural drying and other low-temperature thermal applications.

Future work may extend this study by evaluating alternative PCMs with higher latent-heat capacity and thermal conductivity (e.g., stearic acid, erythritol, or nano-enhanced PCM composites), by performing Computational Fluid Dynamics (CFD) analysis of the airflow and temperature fields within the collector duct, by optimising the aerofoil chord length, thickness ratio, and staggered spacing, and by directly coupling the developed collector to a

drying chamber to evaluate its performance on real agricultural produce such as fruits, vegetables, spices, and food grains under field conditions.

7. References

[1] M. Nagaraj, M. K. Reddy, A. K. H. Sheshadri, and K. V. Karanth, "Numerical analysis of an aerofoil fin integrated double pass solar air heater for thermal performance enhancement," Sustainability, vol. 15, no. 1, p. 591, 2023.

[2] G. Santh et al., "Thermo-hydraulic performance of a solar air heater in an indirect solar dryer with alternative wing structured absorber," J. Renewable Eng., vol. 12, pp. 238–242, 2024.

[3] V. P. Singh, S. Jain, A. Karn, A. Kumar, G. Dwivedi, C. S. Meena, N. Dutt, and A. Ghosh, "Recent developments and advancements in solar air heaters: A detailed review," Sustainability, vol. 14, no. 19, pp. 1–55, 2022.

[4] C. Dosapati et al., "Thermal performance of a packed bed double pass solar air heater with a latent heat storage system: An experimental investigation," Renewable Energy, vol. 145, pp. 1361–1387, 2020.

[5] F. Al-Sulaiman et al., "Thermal analysis of a double-pass solar air heater integrated with a PCM-based thermal storage unit," Energy Convers. Manage., 2020.

[6] M. H. Machi, "Energy-based performance analysis of a double pass solar air collector integrated to triangular shaped fins," Int. J. Energy Environ. Eng., vol. 13, pp. 415–431, 2022.

[7] M. Murali et al., "Experimental comparison of double-pass solar air heaters with longitudinal fins in upper and lower channels," Int. J. Thermal Sci., 2022.

[8] S. Sahu and B. N. Prasad, "Exergy analysis of a solar air heater with arc-shaped wire rib roughness on the absorber plate," Energy, vol. 11, pp. 125–127, 2019.

[9] F. Chabane, N. Hatraf, and N. Moummi, "Experimental study of heat transfer coefficient with rectangular baffle fin of solar air heater," Frontiers in Energy, vol. 8, no. 2, pp. 160–172, 2014.

[10] A. B. Khan et al., "Heat transfer intensification in latent heat thermal storage systems: A review," Renewable Sustainable Energy Rev., 2016.